J Oral Maxillofac Surg
50:969-978, 1992

Evaluation of a Low-Temperature Calcium Phosphate Particulate Implant Material:

Physical-Chemical Properties and In Vivo Bone Response

JOHN L. RICCI, PHD,* NORMAN C. BLUMENTHAL, PHD,†
J.M. SPIVAK, MD,‡ AND H. ALEXANDER, PHD§

A study was conducted to evaluate the osteoconductive ability of a particulate, low-temperature hydroxylapatite (HA^{LT}) material (OsteoGen; Impladent, Holliswood, NY). An implantable chamber model was used to determine the ability of this material to encourage bone ingrowth into channels lined with either rough-surfaced titanium or rough-surfaced plasma-sprayed hydroxylapatite. The HA^{LT} material increased bone ingrowth into the titanium-lined channels comparable with that in plasma-sprayed hydroxylapatite-coated channels. It was incorporated into ingrowing bone without intervening soft tissue, with the bone bonding directly to the material surface in much the same fashion as it bonds at the plasma-sprayed hydroxylapatite surface. Mechanical testing of the ingrown bone showed no weakness because particles were incorporated. At 12 weeks, the particles began to show signs of dissolution. It was concluded that the HA^{LT} material is a biocompatible, osteoconductive material that conducts bone ingrowth in much the same way as high-temperature particulate hydroxylapatite ceramics. This material has the additional desirable property of being slowly resorbable, a beneficial characteristic for many bone-filling applications.

Calcium phosphate materials such as hydroxylapatite (HA) have served as the basis for a variety of dental, maxillofacial, and orthopaedic implants. Hydroxylapatite, $Ca_{10}(PO_4)_6(OH)_2$, the major mineral component of bone, is in fact the idealized, "prototype" compound of biological apatites. As such, it readily accepts substitutional and compositional defects of considerable magnitude that have profound effects on apatite solubility and reactivity. For example, bone mineral consists of a calcium-deficient, microcrystalline, nonstoichiometric HA in which CO_3 is substituted for PO_4 (4% to 6%).[1]

Received from the Department of Bioengineering, Hospital for Joint Diseases Orthopaedic Institute, New York.
* Research Scientist.
† Associate Director.
‡ Research Resident.
§ Director.
Address correspondence and reprint requests to Dr Ricci: Department of Bioengineering, Hospital for Joint Diseases Orthopaedic Institute, 301 East 17th St, New York, NY 10003.

0278-2391/92/5009-0010$3.00/0

Of particular importance as implant materials are the calcium phosphates with calcium/phosphorous ratios of 1.5 to 1.67. Tricalcium phosphate and HA form the lower and upper boundaries, respectively, of this compositional range. Ceramics made from tricalcium phosphates are, in general, rapidly resorbing materials, whereas HA ceramics are more stable.[2] In general, HA ceramics that are formed at high temperatures are more stable than those formed at lower temperatures, a phenomenon related to the effect of temperature on the size of the crystals being formed and, in turn, on the effect of crystal size on solubility.[3] Although it may be questioned whether high-temperature ceramics are technically HA at all (since high-temperature treatment results in a severely hydroxyl-deficient material), natural and ceramic HA are nevertheless sufficiently similar that the synthetic varieties have proven to be extremely biocompatible.

Interaction of HA With Bone

In a review, Jarcho[4] observed that the majority of histologic studies of bone-HA interaction report direct

bony contact between HA and host bone, with apparently little tendency to form soft-tissue encapsulation of the material. Other investigations suggest that a direct bonding exists between HA and host bone.[5,6] Walker and Katz[7] and Denissen et al[8] hypothesized the formation of a chemical bond in the interaction between the organic components and HA of bone on the one hand, and the synthetic HA on the other. The work of Hench[9] on glasses that leach calcium phosphate ions supports this concept of direct bonding. Recent work in the authors' laboratory has shown the existence of a direct chemical bond between bone and HA[10] and suggests that this bond is the result of a combination of cellular production of extracellular matrix components and direct physical-chemical deposition of new HA at the tissue-ceramic interface.[11,12]

Nevertheless, HA is not truly osteogenic; nor is it osteoinductive. (Osteogenesis is the formation of mineralized tissue by osteoblasts; osteoinduction is the phenotypic conversion of soft tissue cells to osseous tissue cells, eg, demineralized bone matrix[13] or bone morphogenic protein[14], by appropriate stimulation.) Autogenous bone graft is osteogenic; it causes the translocation of bone-forming osteoblasts and preosteoblasts to sites where they may synthesize new bone.

Hydroxylapatite, however, is both osteophilic and osteoconductive in much the same way as is devitalized autogenous graft or banked bone. Synthetic HA acts as a trellis for the ingrowth and subsequent deposition of new bone.[15] With devitalized graft or banked bone, the process of replacement with living bone can be extremely slow, as the dead bone must first be resorbed by osteoclastic activity and replaced by "creeping substitution." Most HAs, on the other hand, are not resorbed, but act simply as osteoconductive agents that are integrated into the new osseous tissue.

Stability of HA

Whereas permanence is desirable in some HA applications (eg, to retain bone attachment in implant surface coatings), in other applications (eg, maxillofacial and dental reconstruction) a slowly resorbing HA, one that encourages bone ingrowth and then slowly resorbs, is preferable. Although it is now generally accepted that very dense HA is nonresorbable, some forms, such as plasma-sprayed HA coatings, are capable of being partially resorbed.[12,16] Microporous and macroporous HA materials have been reported to degrade. However, perhaps the most definitive work in this regard, by Klein et al,[2] suggests that all dense synthetic HAs are essentially inert. Jenei et al,[16] studying the resorbability of six commercially available synthetic HAs in buffered lactate, found that all samples released phosphorous and calcium at a relatively high rate for the first 24 to 72 hours (approximately 1 mg/g sample in both cases); over longer time periods, the release rate dropped by more than 90%.

Orthopaedic, Dental, and Maxillofacial Implant Use of HA Ceramics

Plasma-sprayed HA materials are currently used clinically to coat portions of total hip replacements and have been shown to directly bond to human bone.[17-20] Mechanical testing has shown a marked influence of HA coatings on the rate of bone ingrowth and the strength of the interfacial bond.[10,12,20] These results are of particular clinical interest in that postoperative weight bearing might be allowed earlier, reducing the recuperation period. Another orthopaedic application of HA involves the use of blocks of macroporous material. Many animal experiments have been performed with either sintered blocks[21,22] or coralline material hydrothermally converted from the calcium carbonate exoskeleton of coral.[23-27] Although these implant materials have been found to be osteoconductive and capable of filling to varying degrees with ingrown bone, they are weaker than cancellous bone and depend on bone ingrowth to obtain comparable strengths,[25] thus compromising their suitability, in their basic form, for weight-bearing applications.

Porous HA blocks, which must be shaped before implantation, have been used for craniofacial reconstruction.[28] Results have been favorable; bony ingrowth seems to be rapid, and implant retention is not a problem.

Solid, dense forms of HA have been used to repair bone defects in animals[29] and as tooth root implants following extraction.[30-33] These forms of HA, however, allow no bone ingrowth and are difficult to shape at the time of surgery.

The use of several forms of particulate HA in dental applications has also been reported in the literature. These materials consist of irregular and/or porous particles with irregular packing properties and, in some cases, are mechanically weak. Particulate forms of HA have been used primarily in oral surgical procedures to augment the alveolar ridge[34,35] and in periodontal repair.[36] They have also been used experimentally to successfully fill tooth extraction sites in dogs and monkeys.[33,37]

Testing System

The suitability of testing bone response to implant materials using implantable chambers has been established by several studies.[38-43] Whereas chamber construction most commonly involves commercially pure titanium (CP Ti), the present study used ultrahigh-mo-

lecular-weight polyethylene (UHMW PE). Although titanium has found favor because of its proven biocompatibility and apparent osteointegration with surrounding bone,[44-50] its effects (if any) on the processes of bone growth and repair under examination are not fully known. Moreover, the poisoning of HA formation by various ionic metal species, including Ti, has been demonstrated through in vitro testing.[51]

In this study, channels in the implantable chambers were lined with two surface-roughened materials, CP Ti and plasma-HA–coated CP Ti, the former representing a biocompatible but nonosteoconductive surface, the latter an osteoconductive surface. Half the channels of each type were packed with the HA^{LT} material prior to implantation and half were left empty. This permitted testing of the osteoconductive potential of this material for the conduction of bone ingrowth into channels lined with two different materials.

Materials and Methods

The response of intramedullary bone to OsteoGen (Impladent, Holliswood, NY) HA^{LT} was examined using an implantable chamber model with multiple ingrowth channels. The HA^{LT} consists of angular particles and particle aggregates (Fig 1); individual units have a maximum length of 600 μm. This material is made using a relatively low-temperature proprietary process and is not sintered like high-temperature HA ceramics.

Infrared (IR) spectra of HA^{LT} and comparable materials used either in this study (plasma-sprayed high-temperature HA coating) or as reference materials (deproteinated ox bone and room-temperature HA) were performed on a Perkin-Elmer model 1430 ratio recording spectrophotometer. Samples were prepared by grinding with KBr at a 0.5 wt% concentration and then pressed at 10-ton force in a 13-mm–diameter circular disc to yield clear pellets. The IR scans were 200 to 4,000 cm^{-1}, with a slow scan speed for good resolution.

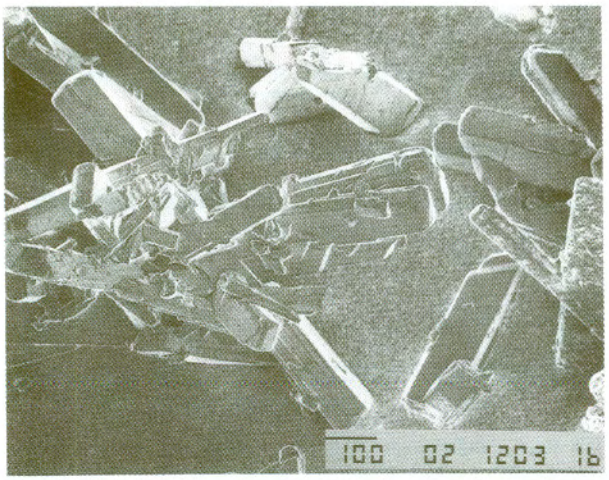

FIGURE 1. Scanning electron micrograph of the HA^{LT} material showing clusters of the particles (bar = 100 μm).

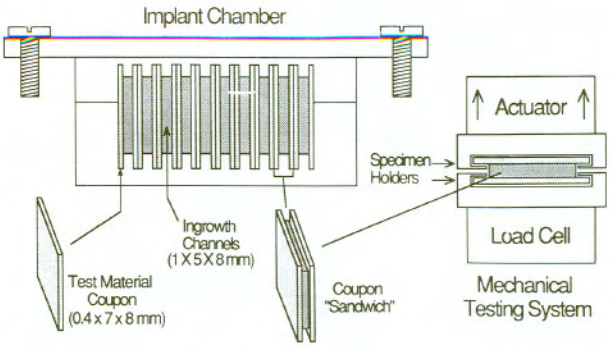

FIGURE 2. Schematic drawings of the assembled implant chamber (front or "open-end" view, with the ingrowth channel openings visible), the coupon-tissue-coupon specimen "sandwich," and the mechanical testing setup used to test intact specimen sandwiches in tension.

Rectangular implant chambers measuring 8 mm wide × 25 mm long × 10 mm deep, and containing a central open area 5 × 18 mm, were machined from medical-grade UHMW polyethylene. Coupons of CP Ti and HA-coated CP, each measuring 7 × 8 × 0.4-mm thick, were washed in an organic solvent and air-passivated. Twenty such test coupons (10 of each, with pairs of one type lining each channel) were placed widthwise along slots cut into the top and bottom of the central space in the polyethylene chamber, thus constituting the primary surfaces lining the 10 ingrowth channels created (Fig 2). Each channel measured 1 × 5 mm at the openings, 8 mm from end to end. A 2-mm lip was present on the outer surface of the UHMW PE implant to seal off the medullary space from potential ingrowth of periosteal new bone. Also, the row of ingrowth channels was offset 2 mm from the outer lip of the implant, so that after implantation they were wholly within the intramedullary canal and not adjacent to any transcortical bone surface. The assembled chambers were gas-sterilized with ethylene oxide and implanted through a longitudinal cortical defect in the lateral metaphysis of the distal femur. After implantation, the ingrowth channels were oriented perpendicular to the long axis of the femur; the channel openings faced the endosteal surface of the intact anterior and posterior cortices (Fig 3).

All operations were performed by a single surgeon, and operative technique was identical for each dog. The supracondylar region of the femur was approached by a direct lateral skin incision extending distally along the lateral border of the patella tendon to the tibial tubercle. After incision of the fascia lata and lateral

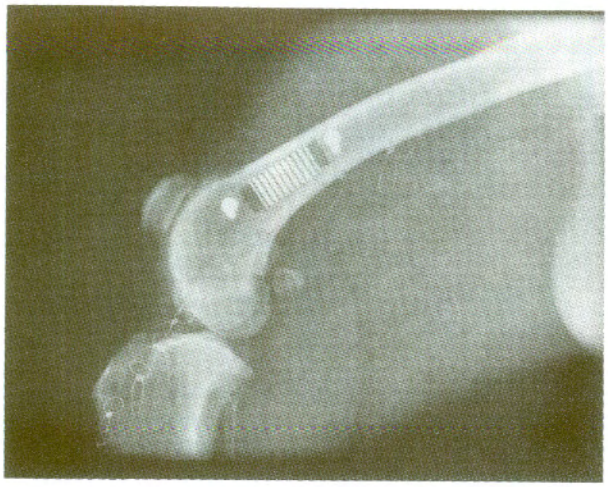

FIGURE 3. Lateral radiograph showing the intramedullary position of the ingrowth channels in situ, 6 weeks postchamber implantation in the lateral distal femur, with the channel openings adjacent to the intact anterior and posterior cortices.

patellar retinaculum, the lateral cortex of the distal femur was reached through the avascular and internervous plane between the vastus lateralis and the lateral hamstrings. The patella was dislocated medially to facilitate the exposure. The lateral periosteum was incised longitudinally, and both anterior and posterior flaps were carefully elevated. A drill template was fixed to the lateral metaphysis using Kirshner wires, and a rectangle measuring 8×25 mm was marked by serial drillholes made with a Ti-coated drillbit. The template was always positioned to allow the most distal placement of the implants in the femoral metaphysis, equidistant between the anterior and posterior cortices. The drillholes were connected with an osteotome, and the lateral cortical window was removed. An osteotome was then used to remove a 10-mm–deep rectangle of cancellous metaphyseal bone flush with the sides of the defect. The sides were carefully enlarged as needed to allow for the snug insertion of a metal trial implant. The blood filling the intramedullary defect was used to fill the channels in the implant so that no air was left in the channels, and the implant was carefully inserted. Unicortical 2.7-mm titanium bone screws (Synthes, Paoli, PA) were used to fix the implant both proximally and distally, preventing any implant motion. Closure was done using interrupted resorbable sutures to repair the fascia lata and patellar retinaculum and to reapproximate the subcutaneous tissue, and interrupted 3-0 stainless steel sutures were used for the skin. Bilateral procedures were done on all animals, which were allowed full postoperative weight bearing. All were given intramuscular antibiotics (penicillin-G procaine) preoperatively and for the first 5 postoperative days.

The study group consisted of four skeletally mature hounds whose implants contained channels lined by either surface-roughened CP Ti or surface-roughened plasma-HA–coated CP Ti. The HA coating consisted of a 50- to 75-μm layer of plasma-sprayed HA (Impladent). In each chamber the 10 channels were lined with the two materials in an alternating fashion. Scanning electron micrographic (SEM) analysis of both coated and uncoated Ti coupons showed a similar surface roughness and general architecture. In each dog, one chamber was implanted "as is," with the intramedullary blood used to fill the channels prior to their insertion as previously described. In the other chamber, all 10 channels were hand-packed intraoperatively with a slurry made by mixing 5 mL of intramedullary blood with 3 g of a sterile HA^{LT} just prior to implantation into the femur. Thus in each dog the two chambers held a total of 20 channels, four sets of five channels in each of the following configurations: Ti-lined and left empty, HA-lined and left empty, Ti-lined and filled with HA^{LT}, and HA-lined and filled with HA^{LT}.

Two dogs each were killed 6 and 12 weeks postoperatively. The femurs were removed intact and kept on ice. A diamond wire saw was then used to isolate each implant from the surrounding bone. Most of the implants were then carefully disassembled, and the contents of the individual channels, consisting of fibrous tissue and newly developed bone that had grown in from the adjacent medullary space, were removed. Representative undecalcified specimens were then fixed in 10% formalin for light microscopy and microradiographic examination. A special effort was made to preserve the two tissue-test coupon interfaces intact for

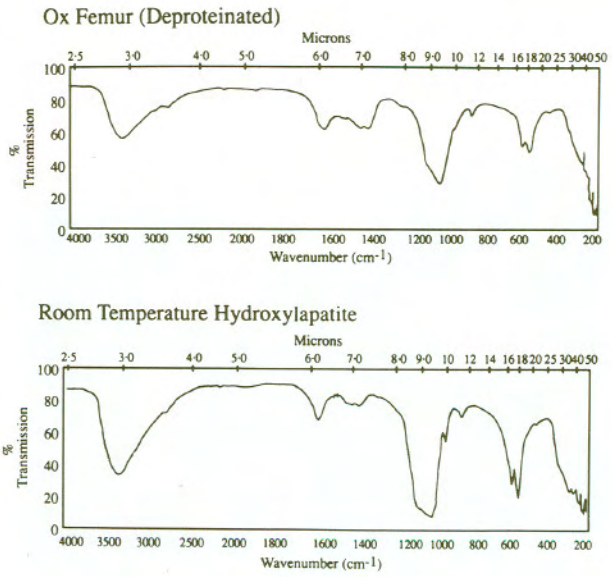

FIGURE 4. Infrared spectra of KBr pellets (0.5%) of ox bone (deproteinated by hydrazine) and HA prepared at room temperature. Note the general similarity of the spectra in CO_3 content (1,450 cm^{-1}), and lack of OH bands (630 and 3,570 cm^{-1}).

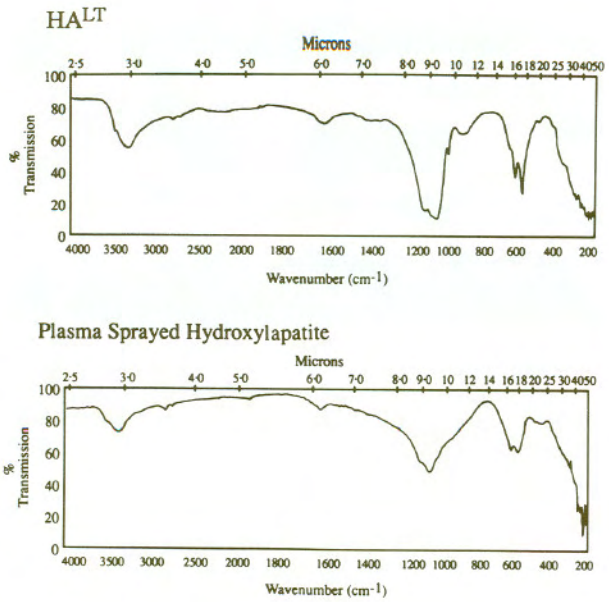

FIGURE 5. Infrared spectra of KBr pellets (0.5%) of HA^{LT} and plasma-sprayed HA. Note the OH bands, as shoulders, at 630 and 3,570 cm^{-1} in the HA^{LT} pattern and the low CO_3 content (1,450 cm^{-1}). By contrast, the spectrum of the plasma-sprayed HA displays an anomalous broadening of the P-O stretching band at 1,000 to 1,100 cm^{-1}, with no CO_3 bands (1,450 cm^{-1}).

each ingrowth channel. All specimens were maintained on ice and moistened with normal saline as needed. When it was determined that the entire coupon-tissue-coupon "sandwich" had maintained its integrity at all interfaces, it was carefully placed into a custom holding jig (Fig 2) and mechanically tested to failure in tension using an Instron servohydraulic testing system at a rate of 2.5% displacement per second. The failure surfaces of representative specimens were examined by SEM following mechanical testing. Following fixation in phosphate-buffered glutaraldehyde, the specimens were critical-point-dried, sputter-coated with a 200-Å–thick layer of gold, and examined using a JEOL JSM T-300 scanning electron microscope.

Some undisturbed specimens (with adjacent coupons intact) were fixed in 10% formalin and embedded in methyl methacrylate. Undecalcified sections of these specimens were examined by microradiography and by light microscopy following staining with hematoxylin and eosin or by the Masson trichrome or von Kossa techniques.

Results

Infrared Analysis

The infrared spectrum of bone mineral (deproteinated ox bone; Fig 4) clearly shows CO_3 bands in the neighborhood of 1,450 cm^{-1}. This substitution of CO_3 for PO_4 is typical of biological apatites. Similar CO_3 bands are seen in the spectra of a precipitated HA made at room temperature under ambient CO_3 conditions (Fig 4). The spectra of these two apatites are similar to the extent of the CO_3 substitution in both. The spectrum of HA^{LT} shows very little CO_3 absorption at 1,450 cm^{-1} (Fig 5). In addition, at 630 and 3,570 cm^{-1} the HA^{LT} clearly shows the presence of the OH absorption bands that are not visible in the spectrum of the bone and precipitated HA. Otherwise, the spectra of HA^{LT} resembles that of precipitated HA. By contrast, the spectrum of plasma-sprayed HA shows an anomalous broadening of the PO_4 stretching mode not present in the spectra of the other three materials. The CO_3 bands at 1,450 cm^{-1} are essentially absent in this spectrum (Fig 5).

General Pattern of Bone Ingrowth

Bone and soft tissue ingrowth occurred from the two open ends of each channel. The new bone was the result of primary formation, with no evidence of intermediate cartilage formation. This bone originated from, and was continuous with, the intramedullary bone adjacent to the chamber. It began as the formation of thin trabeculae consisting primarily of immature woven bone that grew into the open ends of the channels and progressed into the thin connective tissue that initially filled the channel. Marrow elements were present in the intertrabecular spaces. Both the bone and soft tissue exhibited more mature characteristics at 12 weeks than at 6 weeks. By 12 weeks the trabeculae had progressed

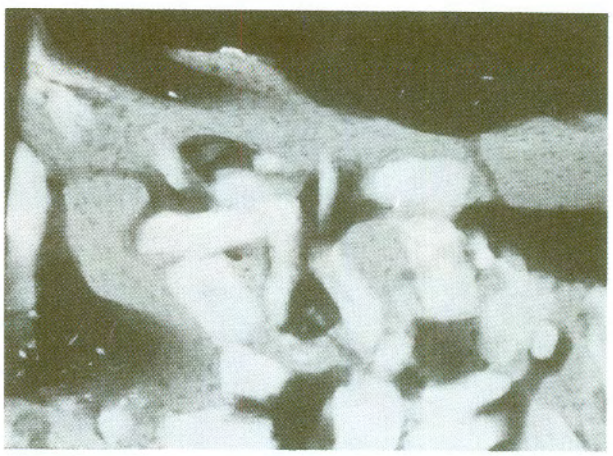

FIGURE 6. Microradiograph of bone ingrowth into an HA^{LT}-filled, Ti-lined channel at 6 weeks, showing small amounts of bone contact along the upper border (where the Ti plate was removed), and extensive incorporation of HA^{LT} particles into the ingrowing bone (original magnification × 212).

further into the channels and had thickened and exhibited lamellar remodeling. In some areas the bone had thickened to form structures similar to osteons. By 12 weeks the remaining connective tissue had also matured, becoming less cellular and more organized. Whereas this general pattern of bone and soft tissue ingrowth was apparent in all channels, there were differences in the amounts of bone ingrowth and the interaction of the bone with the channel walls and contents.

Effects of HA^{LT} Packing and Wall Composition on Bone Ingrowth

At 6 weeks postimplantation, all the empty HA-plasma-coated channels contained larger amounts of radiographically visible ingrown bone than those channels lined with uncoated CP Ti, regardless of the anatomic position of the channel within the implant chamber. The presence of the HA^{LT} grouting within the channel seemed significantly to enhance the ingrowth of bone in the CP-Ti–lined channels. In the plasma-HA coated channels, the presence of HA^{LT} did not significantly enhance or block the increased bone ingrowth seen at 6 weeks. Histologically, a 50- to 100-μm layer of fibrous tissue was seen at the coupon surface in the 6-week CP Ti specimens. The ingrown bone was shown to incorporate the HA^{LT} grouting and form direct attachment to the particles (Figs 6, 7). The ingrown bone consisted of thin trabeculae vascular woven bone, surrounded on most of their surfaces by osteoid tissue and numerous osteoblasts. The plasma-HA–coated channels showed direct bone attachment to the HA coating at the light microscopic level (Fig 7). Histological examination of bone interaction with both the HA coating and the HA^{LT} materials showed bone directly surrounding and attaching to these materials without any visible interposing tissue.

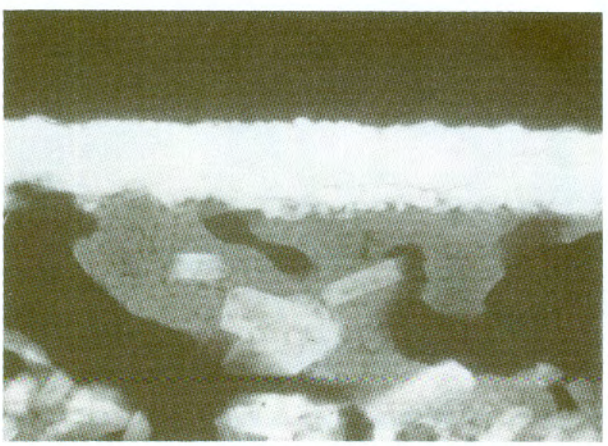

FIGURE 7. Microradiograph of bone ingrowth into an HA^{LT}-filled, HA-lined channel at 6 weeks showing extensive bone attachment to both the HA lining and the HA^{LT} particles (original magnification ×212).

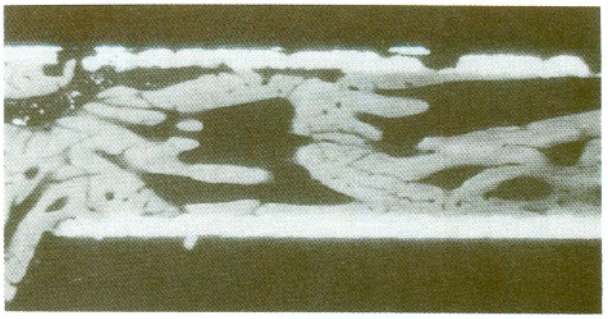

FIGURE 8. Microradiograph of bone ingrowth into an unfilled HA-lined channel at 12 weeks showing extensive ingrowth and consistent bone attachment to the HA coating (original magnification ×33).

At 12 weeks, radiographic examination of the chambers showed a complete bridge of bone within the HA-coated channels with or without the HA^{LT} material, regardless of the anatomic position of the channel (Fig 8). The CP titanium channels showed greater bone ingrowth than in the 6-week dogs (Fig 9), but displayed complete bridging by new bone in less than half of the channels. The presence of the HA^{LT} grouting within the channels significantly enhanced bone ingrowth in the CP Ti channels, promoting complete filling of all channels with new bone (Fig 9). Microradiographic and histological examination confirmed the 6-week observation of ingrown bone directly attaching to the HA coating as well as to the HA^{LT} material (Fig 10). In the CP Ti chambers, the thick fibrous tissue separating the ingrown bone from the coupon surface at 6 weeks was not found, and in many areas no intervening tissue was visible at the edges of the samples examined. In most areas, however, the ingrown bone was separated from the channel wall by a thin layer of loose connective tissue, at most only a few cell layers thick.

At 12 weeks, the central connective tissue seemed mature and well-oriented and was intimately associated with and oriented to the ingrown bone. Osteoid was seen on less of the trabecular surfaces than in earlier time periods, and larger areas of mature lamellar bone with fewer marrow spaces were found.

Scanning electron micrographic analysis of fractured specimens at 12 weeks showed evidence of direct bone trabeculae attachment to the plasma-sprayed HA coating and to the HA^{LT} particles. These fractured samples showed HA^{LT} particles embedded or encased in bone trabeculae (Fig 11). Some particles showed coatings of cells and extracellular matrix (Figs 11, 12). Many particles also showed surface pitting and rounded corners indicative of slow dissolution (Fig 13).

Twenty-five plasma-HA–coated channel specimens (13 containing HA^{LT}) and 6 CP Ti channel specimens

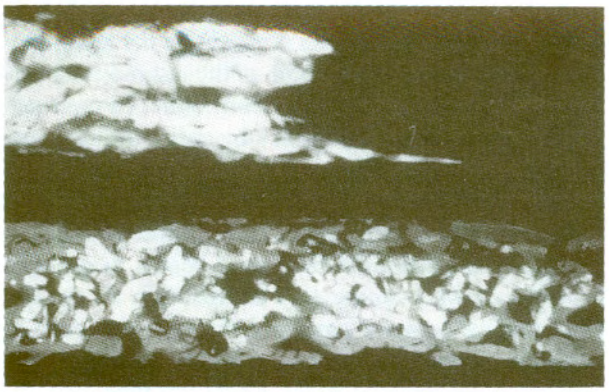

FIGURE 9. Microradiograph (for comparison with Fig 8) of bone ingrowth into CP-titanium–lined channels at 12 weeks, with (below) and without (above) the presence of HA^{LT} grouting. By 12 weeks, much more ingrowth is noted in the HA^{LT}-filled channel (original magnification ×33).

(5 containing HA^{LT}) were mechanically tested in tension to determine the adhesion strength between the chamber walls and the ingrown tissue. The plasma-HA–coated specimens included 1) 10 samples at 6 weeks, 5 of which included HA^{LT} grouting within the channels; and 2) 15 samples at 12 weeks, 8 including grouting. All six CP Ti samples tested were 12-week, and all but one included grouting. The reason only six CP Ti channels could be tested was that at least one of the coupon-bone interfaces of most of these samples (including all of the 6-week samples) became disrupted by the minimal manipulation necessary to remove the intact specimens from the polyethylene chambers. This indicated that the adhesion strengths in these samples was close to zero. One 12-week CP Ti sample was tested and failed at 3.66 N, and the 5 CP Ti specimens with HA^{LT} grouting failed at an average of 8.88 N (standard deviation ±6.4). The five 6-week unfilled plasma-HA–coated samples failed at 15.29 N (±3.03), and the seven 12-week samples failed at 44.81 N (±15.54). Of the plasma-HA–coated channels with HA^{LT} grouting tested, the five 6-week samples failed at 23.00 N (±16.32), and the eight 12-week samples failed at an average of 35.56 N (±18.99).

Statistical analysis using unpaired *t*-tests showed no significant difference in failure strengths according to presence or absence of the HA^{LT} grouting in the plasma-HA–coated specimens at both 6 and 12 weeks. A significant increase ($P < .01$) was found in failure strengths of the plasma-HA–coated specimens at 12 weeks compared with the 6-week samples.

Discussion

The spectrum of ox bone mineral shows a typical pattern of mammalian bone, with significant CO_3 content and a low splitting of the PO_4 antisymmetric bending mode at 550 to 600 cm^{-1} caused by the distortion in the apatite lattice induced by the substitution of CO_3 for PO_4. The organic collagen bands were not visible because the sample was hydrazine-deproteinated. The absence of the OH bands at 630 and 3,570 cm^{-1} is because of small crystal size and the CO_3 content and not to the near-total absence of structural OH.[1] The spectrum of a control HA precipitated under ambient conditions is quite similar to that of bone, with roughly the same CO_3 content. The OH bands are absent from the spectrum for similar reasons.[1] The spectrum of the HA^{LT} material indicates an apatite prepared at somewhat above body temperature (perhaps 60° to 80°C), when it is precipitated from aqueous solution. This is evident from the greater splitting of the PO_4 bending at 550 to 600 cm^{-1} and the absence of CO_3 bands at 1,450 cm^{-1}. At 630 and 3,570 cm^{-1}, OH bands can be seen, which is consistent with a higher preparation temperature. Overall, HA^{LT} is a somewhat better-crystalized apatite than bone mineral, but is not drastically different in structure. In addition, a powder x-ray diffraction study of the HA^{LT} material confirmed the infrared analysis and indicated that no phases other than crystalline HA were present.

By contrast, the spectrum of the high-temperature plasma-sprayed HA is notably different from those of the other three apatites. The splitting of the PO_4 bending mode at 550 to 600 cm^{-1} is considerably less than that of the other apatites despite the lack of any CO_3 bands at 1,450 cm^{-1}. With the greatly broadened PO_4 stretching mode at around 1,050 cm^{-1}, one sees the most striking differences between this high-temperature plasma-sprayed HA and the other apatites precipitated

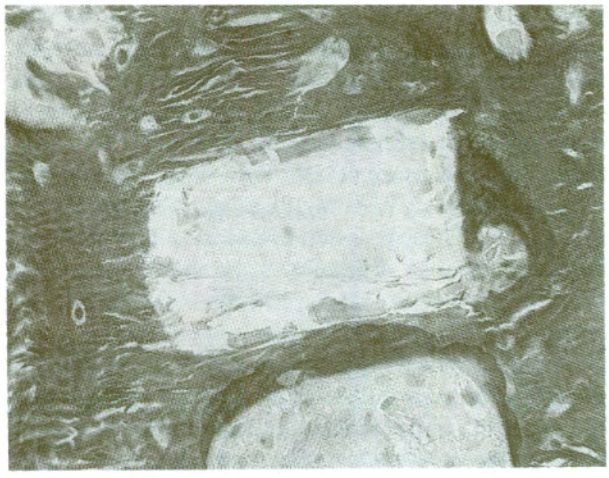

FIGURE 10. Photomicrograph showing an HA^{LT} particle (clear rectangular space) surrounded by bone without any intervening soft-tissue layer. Dark-staining osteoid (to right and below particle) is also shown adjacent to the HA^{LT} particle. Although the brittle HA was fragmented by the microtome during the slide preparation, the fragments adjacent to surrounding bone, seen at the periphery of the space left by the particles, remain attached. This reflects the strength of the bond between HA^{LT} and bone (Masson stain, original magnification ×529).

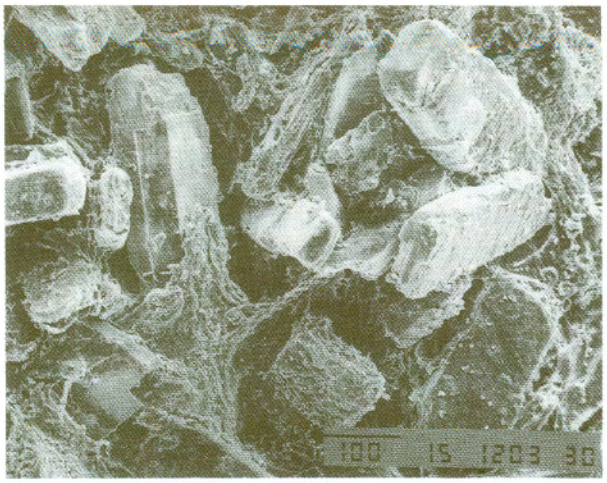

FIGURE 11. Scanning electron micrograph of a 12-week sample fractured from mechanical testing showing HA^{LT} particle incorporation into the bone as well as tissue and cellular elements coating some particles (bar = 100 μm).

from aqueous medium, whether in vitro or in vivo. The cause of this anomalous broadening, although not completely understood, probably involves some significant specific structural distortion in the lattice not present in low-temperature precipitated apatites. Also, no OH bands are present, which is not surprising given the high temperature (above 1,000°C) and high vacuum conditions of preparation. The properties of this material are very different from those of biological and precipitated apatites.

The use of the implantable chamber model for testing bone response to synthetic materials is justified on the basis that this experimental model permits measurement of differences in the affinity of bone for various test materials by evaluating the speed, amount, and quality of bone ingrowth. This model also allows for a detailed analysis of the bone-implant interface. It was designed to emulate the in vivo location of orthopaedic implants more closely than other models currently used to study bone ingrowth, eg, the transcortical plug model.[52-61] In the latter, cylinders of test materials are placed through drillholes in the diaphysis of long bones. Specimens are analyzed both histologically, to examine the extent of bone ingrowth in porous specimens and to view the bone-implant interface, and mechanically, by pushout testing of the shear strength and stiffness of the bone-implant interface. Because the response in the transcortical plug model is primarily one of cortical bone, it cannot realistically simulate bone response to implants that are primarily in contact with trabecular bone. That a truly intramedullary bone response was observed in the present study is indicated by the fact that bone ingrowth into the channels was found to be symmetrical across the channel openings, with equal amounts of bone ingrowth into the most superficial and the deepest edges of the channels.

In the present model, only the openings of the ingrowth channels are placed adjacent to the intramedullary endosteal bone; the bulk of the test material surfaces is initially at a distance from bone. In contrast, in the transcortical plug model the entire implant surface is initially in direct contact with bone. The ingrowth channels in the present model first fill with blood, which is rapidly organized to a loose connective tissue at the same time that bone begins to grow in from the channel openings. A competition for the implant surface between bone and fibrous tissue ensues, and material properties and surface properties of the channel walls combine to favor one cell type over the other.

In the present experiment, both HA^{LT} and the plasma-sprayed HA material decisively encouraged bone ingrowth, exhibiting clear osteoconductive properties singly as well as in combination. The presence of the HA^{LT} material within the ingrowth channel, even in the absence of a bone-enhancing coating on the metal, was associated with a large increase in bone ingrowth versus unfilled channels having identical Ti lining coupons. The mechanical testing of these specimens indicated that the HA^{LT} material was firmly incorporated into the bone and that it did not act as a weak point for fracture initiation. In addition, the 12-week specimens showed signs of mild dissolution of the HA^{LT} material. These results underscore certain characteristics of the HA^{LT} material:

1. It is clearly an osteoconductive material that promotes bone ingrowth into defects through bone attachment and conduction from particle to particle in similar fashion to other reported HA particulates.
2. It does not seem to act as a stress riser in mechanically tested specimens, indicating that the

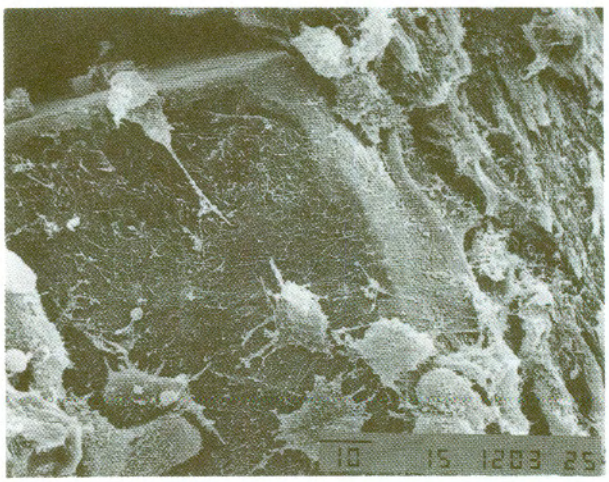

FIGURE 12. Scanning electron micrograph showing an HA^{LT} particle from a 12-week mechanical-tested specimen. Note the thin extracellular matrix coating with attached cells (bar = 10 μm).

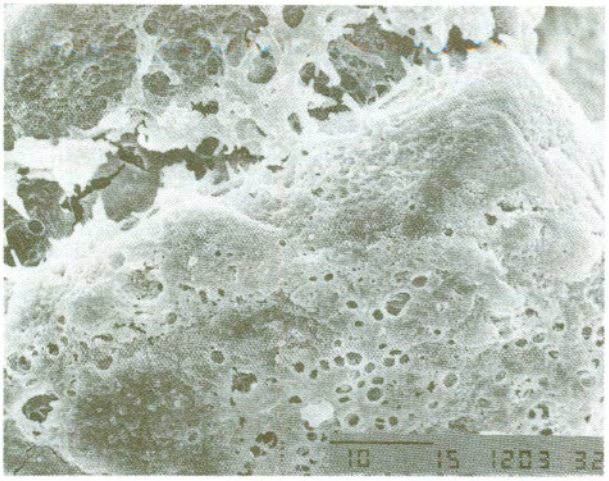

FIGURE 13. Scanning electron micrograph showing an HA^{LT} particle from a 12-week mechanical-tested specimen. The surface pitting and the smoothing of the corner of the particle indicate dissolution (bar = 10 μm).

particles have adequate mechanical strength and that their attachment to surrounding bone is strong.

3. It shows signs of slow dissolution. This is in significant contrast with other particulate HA materials, most of which are high-temperature materials, relatively stable, and thus considered permanent in nature.

Conclusion

Both HA^{LT} (OsteoGen) and plasma-sprayed HA coatings promote increased bone in-growth at both 6 and 12 weeks in this model. In contrast with the roughened-surface Ti test material, which was well tolerated but not osteoconductive, both HA materials were osteoconductive. The HA^{LT} material is directly incorporated into ingrown bone, shows no indication of mechanical weakness, and shows signs of slow dissolution at 12 weeks. Because it is biologically osteoconductive and, by virtue of its physical-chemical characteristics, similar to bone mineral in its potential ability to dissolve over time and be replaced by bone, this material is an attractive bone substitute material.

Acknowledgment

The authors wish to thank Dr Foster Betts of the Hospital for Special Surgery, New York City, for the x-ray diffraction analysis of the HA^{LT} material.

References

1. Posner AS, Betts F, Blumenthal NC: Chemistry and structure of precipitated hydroxylapatites, *in* Nriagu JO, Moore PB (eds): Phosphate Minerals. New York, NY, Springer-Verlag, 1984, pp 330-350
2. Klein CP, Driessen AA, de Groot K, et al: Biodegradation behavior of various calcium phosphates. J Biomed Mater Res 17:769, 1983
3. Driessens FCM: Formation and stability of calcium phosphates in relation to the phase composition of the mineral in calcified tissues *in* de Groot K (ed): Bioceramics of Calcium Phosphate. Boca Raton, FL, CRC, 1983, pp 1-32
4. Jarcho M: Calcium phosphate ceramics as hard tissue prosthetics. Clin Orthop 157:259, 1981
5. Jarcho M, Kay JF, Gumaer KI, et al: Tissue cellular and subcellular events at a bone-ceramic hydroxylapatite interface. J Bioeng 1:79, 1977
6. Walker MM, Katz JL: Interfacial osteogenesis on calcite surfaces. Transactions of the 30th Annual Meeting of the Orthopaedic Research Society, vol 9, Atlanta, GA, 1984, p 122
7. Walker MM, Katz JL: Mechanisms for the bonding of bone to dense hydroxylapatite. Transactions of the Second World Congress on Biomaterials, vol 7, Washington, DC, 1984, p 152
8. Denissen JW, deGroot K, Makkes PC, et al: Tissue response to dense apatite implants in rats. J Biomed Mater Res 14:713, 1980
9. Hench LL: Bioactive implants. Transactions of the 11th Annual Meeting of the Society for Biomaterials, 1985, p 25
10. Spivak JM, Ricci JL, Blumenthal NC, et al: A new canine model to evaluate the biological response of intramedullary bone to implant materials and surfaces. J Biomed Mater Res 24:1121, 1990
11. Blumenthal N, Ricci JL, Alexander H: The effects of implant surfaces on bone mineral formation and attachment in vitro. Transactions of the 15th Annual Meeting of the Society for Biomaterials, vol 12, Lake Buena Vista, FL, 1989
12. Ricci JL, Spivak JM, Chang J-H, et al: Mechanical and morphological characterization of bone interaction with titanium and hydroxylapatite-coated titanium using an implantable chamber system. Transactions of the 37th Annual Meeting of the Orthopaedic Research Society, vol 10, Anaheim, CA, 1991
13. Glowacki J, Kaban LB, Sonis ST, et al: Physiological aspects of bone repair using demineralized bone *in* Hunt TK, et al (eds): Soft and Hard Tissue Repair. New York, NY, Praeger, 1984
14. Urist MR, deLange RJ, Finerman GAM: Bone cell differentiation and growth factors: Induced activity of chondro-osteogenic DNA. Science 220:6680, 1983
15. Simmons DJ: Fracture healing *in* Urist MR (ed): Fundamentals and Clinical Bone Physiology. Philadelphia, PA, Lippincott, 1980, pp 136-178
16. Jenei SR, Bajpai PK, Salsbury RL: Resorbability of commercial hydroxylapatites in lactate buffer. Transactions of the 2nd Annual Scientific Session, Academy of Surgical Research, 1986
17. Hardy DCR, Frayssinet P, Guilhem A, et al: Bonding of hydroxylapatite-coated femoral prostheses. J Bone Joint Surg [Br] 73:732, 1991
18. Furlong RJ, Osborn JF: Fixation of hip prostheses by hydroxylapatite ceramic coatings. J Bone Joint Surg [Br] 73:741, 1991
19. Thomas KA, Cook SD, Anderson RC, et al: Biological response to hydroxylapatite coated porous titanium hips. Transactions of the 12th Annual Meeting of the Society for Biomaterials, vol 9, Minneapolis, MN, 1986, p 15
20. Ducheyne P, Hench LL, Kagan A Jr, et al: Effect of hydroxylapatite impregnation on skeletal bonding of porous coated implants. J Biomed Mater Res 14:225, 1980
21. Hoogendoorn HA, Renooij W, Akkermans LMA, et al: Long-term study of large ceramic implants (porous hydroxylapatite) in dog femora. Clin Orthop 187:281, 1984
22. Patka P, Driessen AA, de Groot K, et al: Segmental bone defect repair with hydroxylapatite in weight-bearing models. Transactions of the Second World Congress on Biomaterials, Annual Meeting of the Society for Biomaterials, vol 7, Washington, DC, 1984, p 245
23. Chiroff RT, White EW, Webber JN, et al: Tissue ingrowth of replamineform implants. J Biomed Mater Res 9:29, 1975
24. Holmes RE: Bone regeneration within a coralline hydroxylapatite implant. Plast Reconstr Surg 63:626, 1979

25. Holmes RE, Tencer AF, Carmichael TW, et al: Mechanical properties of synthetic hydroxylapatite for cancellous bone grafting. Transactions of the 29th Annual Meeting of the Orthopaedic Research Society, 1983, p 67
26. Holmes RE, Bucholz RW, Mooney V: Porous hydroxylapatite as a bone graft substitute in metaphyseal defects: A histometric study. J Bone Joint Surg (Am) 68:904, 1986
27. Shimazaki K, Mooney V: Comparative study of porous hydroxylapatite and tricalcium phosphate as bone substitute. J Orthop Res 3:301, 1985
28. Saylor K, Holmes R, Johns D: Replamineform porous hydroxylapatite as bone substitute in craniofacial osseous reconstruction. J Dent Res 56:173, 1977
29. Boyne PJ, Fremming BD, Walsh R, et al: Evaluation of ceramic hydroxylapatite in femoral defects. J Dent Res 57:108, 1978
30. Denissen HW, de Groot K: Immediate dental root implants from synthetic dense calcium hydroxylapatite. J Prosthet Dent 42: 551, 1979
31. Sage BE, Mehlisch DR, Gumaer KI, et al: Evaluation of solid durapatite to restore atrophic alveolar ridges. Transactions of the 10th Annual Meeting of the Society for Biomaterials, vol 7, Washington, DC, 1984, p 215
32. Kangvonkit P, Matukas VJ, Castleberry DJ: An evaluation of durapatite submerged-root implants for alveolar bone preservation. Transactions of the 13th Annual Meeting of the Society for Biomaterials, vol 10, New York, NY, 1987, p 13
33. Block MS, Kent JN: A comparison of particulate and solid root forms of hydroxylapatite in dog extraction sites. J Oral Maxillofac Surg 44:844, 1985
34. Cranin AN, Gelbman J, Tobin G, et al: Hydroxylapatite (H/A) particulate vs. cones as post-extraction implants in humans. Transactions of the 12th Annual Meeting of the Society for Biomaterials, vol 9, Minneapolis, MN, 1986, p 151
35. Frame JW, Brady CL: Augmentation of an atrophic edentulous mandible by interpositional grafting with hydroxylapatite. J Oral Maxillfac Surg 42:89, 1984
36. Councils on Dental Materials, Research, and Therapeutics, American Dental Association: Hydroxylapatite, beta tricalcium phosphate, and autogenous and allogeneic bone for filling periodontal defects, alveolar ridge. J Am Dent Assoc 108:822, 1984
37. Boyne PJ, Stringer DE, Sheer PM: The use of porous HA particulate implants in fresh extraction sockets to maintain alveolar bone height. Transactions of the 12th Annual Meeting of the Society for Biomaterials, vol 9, Minneapolis, MN, 1986, p 38
38. Albrektsson T: Implantable devices for long-term vital microscopy of bone tissue. Crit Rev Biocompat 3:25, 1987
39. Winet H, Albrektsson T: Wound healing in the bone chamber. 1. Neoosteogenesis during transition from the repair to the regenerative phase in the rabbit tibial cortex. J Orthop Res 6: 531, 1988
40. Kalëbo P, Jacobsson M: Recurrent bone regeneration in titanium implants: Experimental model for determining the healing capacity of bone using quantitative microradiography. Biomaterials 9:295, 1988
41. Benedict JJ, Prewett AB, Kern MN, et al: The evaluation in primates of a bovine derived osteogenic factor using the analytical bone implant model. Transactions of the 15th Annual Meeting of the Society for Biomaterials, vol 12, Lake Buena Vista, FL, 1989, p 125
42. Albrektsson T, Linder L: A method for in vivo observations of the cement-bone interface. Transactions of the First World Congress on Biomaterials, 6th Annual Meeting of the Society for Biomaterials, vol 3, Vienna, Austria, 1980, p 140
43. H Winet JY, Bao R, Moffat R: Control-control bone chamber model for quantitative evaluation of cortical bone primary healing. Transactions of the Orthopaedic Research Society, vol 14, Las Vegas, NV, 1989, p 563
44. Lemons JE, Wiemann MW, Weiss AB: Biocompatibility studies on surgical grade titanium, cobalt, and iron based alloys. J Biomed Mater Res 7:549, 1976
45. Williams DF: Titanium and titanium alloys *in* Williams DF (ed): Biocompatibility of Clinical Implant Materials, vol I. Boca Raton, FL, CRC, 1981
46. Albrektsson T, Brånemark P-I, Hansson H-A, et al: Osseointegrated titanium implants. Acta Orthop Scand 52:155, 1981
47. Linder L, Albrektsson T, Brånemark P-I, et al: Electron microscopic analysis of the bone-titanium interface. Acta Orthop Scand 54:45, 1983
48. Albrektsson T, Hansson H-A, Ivarsson B: Interface analysis of titanium and zirconium bone implants. Biomaterials 6:97, 1985
49. Albrektsson T, Hansson H-A: An ultrastructural characterization of the interface between bone and sputtered titanium or stainless steel. Biomaterials 7:201, 1986
50. Johansson C, Lausmaa J, Ask M, et al: Ultrastructural differences of the interface zone between bone and Ti-6Al-4V or commerically pure titanium. J Biomed Eng 11:3, 1989
51. Blumenthal NC, Cosma V: Inhibition of apatite formation by titanium and vanadium ions. J Biomed Mater Res 23:13, 1989
52. Geesink RGT, De Groot K, Klein CPAT: Chemical implant fixation using hydroxyl-apatite coatings. Clin Orthop 225:147, 1987
53. Anderson RC, Cook SD, Weinstein AM, et al: An evaluation of skeletal attachment of LTI pyrolytic carbon, porous titanium, and carbon-coated porous titanium implants. Clin Orthop 182:242, 1984
54. Geesink RGT, de Groot K, Klein CPAT: Bonding of bone to apatite-coated implants. J Bone Joint Surg [Br] 70:17, 1988
55. Cook SD, Thomas KA, Kay JF, et al: Hydroxylapatite-coated titanium for orthopedic implant applications. Clin Orthop 232:225, 1988
56. Cook SD, Thomas KA, Kay JF, et al: Hydroxylapatite-coated porous titanium for use as an orthopedic biologic attachment system. Clin Orthop 230:303, 1988
57. Bobyn JD, Pilliar RM, Cameron HU, et al: The optimum pore size for the fixation of porous-surfaced metal implants by the ingrowth of bone. Clin Orthop 150:263, 1980
58. Cook SJ, Walsh KA, Haddad RJ Jr: Interface mechanics and bone growth into porous Co-Cr-Mo alloy implants. Clin Orthop 193:271, 1985
59. Thomas KA, Cook SD: An evaluation of variables influencing implant fixation by direct bone apposition. J Biomed Mater Res 19:875, 1985
60. Magee FP, Longo JA, Hedley AK: The effect of age on the interface strength between porous coated implants and bone. Transactions of the 35th Annual Meeting of the Orthopaedic Research Society, vol 14, Las Vegas, NV, 1989, p 575
61. Thomas KA, Kay JF, Cook SD, et al: The effect of surface macrotexture and hydroxylapatite coating on the mechanical strengths and histologic profiles of titanium implant materials. J Biomed Mater Res 21:1395, 1987